Comparisons and Applications of Two-Fluid Plasma Algorithms

B. Srinivasan[*] and U. Shumlak [†]

Aerospace and Energetics Research Program, University of Washington, Seattle, Washington 98195-2250

A. Hakim[‡]

Tech-X Corporation, Boulder, Colorado 80303

This paper describes a study of the five-moment two-fluid plasma model and the asymptotically approximated fluid model that is derived from it. The two models are compared for applications of an electromagnetic plasma shock, magnetic reconnection and an axisymmetric Z-pinch. The physics captured is compared between these fluid models to determine the regime of applicability. These models are explored for their ability to capture small-scale physics with two-fluid effects that are not sufficiently captured by ideal-MHD.

Nomenclature

t	Time variable
Δx	Size of grid cells in x-direction
q_s	Charge of species
m_s	Mass of species
γ	Gas constant
μ_0	Permeability of free space
ε_0	Permittivity of free space
n_s	Number density of species
ρ_s	Mass density of species
$\mathbf{u}_s$	Velocity vector of species
p_s	Pressure of species
ϵ_s	Energy of species
$\mathbf{J}$	Total current density vector
$\mathbf{J_s}$	Current density vector of species
$\mathbf{E}$	Electric field vector
$\mathbf{B}$	Magnetic field vector
k	Wave number
r_{Ls}	Larmor radius of species
δ_s	Skin depth of species
ω_{cs}	Cyclotron frequency of species
v_A	Alfven velocity
v_W	Whistler wave speed
Subscript	
s	species, i for ions and e for electrons

---

[*]Graduate Student, AIAA member
[†]Professor, AIAA senior member
[‡]Research Scientist

American Institute of Aeronautics and Astronautics

I. Introduction

In plasma modeling, there are a number of algorithms that are used to simulate plasma behavior. Ideal Magnetohydrodynamics (MHD) and resistive MHD are among the most commonly used algorithms. Particle codes are also used extensively to model plasmas by including the kinetic effects which are lost in some of these fluid models.

This paper describes a study of the two-fluid plasma algorithm and a reduced fluid model that can be derived from it. The two-fluid plasma model is a five-moment system derived from the Vlasov equation. Euler equations are used to model electron and ion fluids and the full set of Maxwell's equations are used to evolve the electric and magnetic fields.

Asymptotic approximations are applied to the full two-fluid plasma algorithm to obtain Hall-MHD. These asymptotic approximations include setting the speed of light to infinity, neglecting electron inertia and assuming quasi-neutrality. This regime of fluid models is studied and compared to ideal-MHD. Hall-MHD is also classified as a two-fluid model in this paper because it includes the two-fluid effects contained in the Hall term and the diamagnetic drift term. Two-fluid effects become significant when the characteristic spatial scales are small compared to the ion skin depth and the characteristic time scales are short compared to the inverse ion cyclotron frequency.

The full two-fluid plasma model is compared to Hall-MHD for applications of the electromagnetic plasma shock, magnetic reconnection and an axisymmetric Z-pinch. The models are compared for their ability to capture two-fluid physics that occur at small spatial and temporal scales.

The WARPX (Washington Approximate Riemann Plasma) code developed at the University of Washington is used to perform the simulations.

II. Plasma fluid models and the numerical method

II.A. Two-fluid plasma model

The full two-fluid plasma model[1] is described using the Euler equations for the electron and ion fluids

$$\frac{\partial \rho_s}{\partial t} + \nabla \cdot (\rho_s \mathbf{u}_s) = 0 \tag{1}$$

$$\frac{\partial \rho_s \mathbf{u}_s}{\partial t} + \nabla \cdot (\rho_s \mathbf{u}_s \mathbf{u}_s + \nabla p_s \mathbf{I}) = \frac{\rho_s q_s}{m_s} (\mathbf{E} + \mathbf{u}_s \times \mathbf{B}) \tag{2}$$

$$\frac{\partial \epsilon_s}{\partial t} + \nabla \cdot ((\epsilon_s + p_s)\mathbf{u}_s) = \frac{\rho_s q_s}{m_s} \mathbf{u}_s \cdot \mathbf{E} \tag{3}$$

where subscript, s, denotes electron or ion species and the energy is defined as

$$\epsilon_s \equiv \frac{p_s}{\gamma - 1} + \frac{1}{2}\rho_s u_s^2. \tag{4}$$

Maxwell's equations are used to evolve the electric and magnetic fields

$$\frac{\partial \mathbf{B}}{\partial t} + \nabla \times \mathbf{E} = 0 \tag{5}$$

$$\frac{1}{c^2}\frac{\partial \mathbf{E}}{\partial t} - \nabla \times \mathbf{B} = \mu_0 \mathbf{J} \tag{6}$$

$$\nabla \cdot \mathbf{E} = \frac{\varrho_c}{\varepsilon_0} \tag{7}$$

$$\nabla \cdot \mathbf{B} = 0 \tag{8}$$

where $c = (\mu_0 \varepsilon_0)^{-1/2}$ is the speed of light and ϱ_c and $\mathbf{J}$ are the charge density and the current density defined by

$$\varrho_c \equiv \sum_s \frac{q_s}{m_s}\rho_s \tag{9}$$

$$\mathbf{J} \equiv \sum_s \frac{q_s}{m_s}\rho_s \mathbf{u}_s. \tag{10}$$

American Institute of Aeronautics and Astronautics

In the five moment, two-fluid plasma model, the characteristic speeds include the fluid speeds of sound and the speed of light. Resolving the speed of light, which is the fastest characteristic speed in the system, allows small spatial- and temporal-scale physics to be captured. The speed of light restricts the time step.

II.B. Hall-MHD

Three asymptotic approximations are applied to the full two-fluid model described previously. These include setting the speed of light to infinity, neglecting electron inertia and assuming quasi-neutrality. The ion fluid is still described by the Euler equations, Eqs. (1)–(3).

The quasi-neutrality assumption eliminates the electron continuity equation and $n_e = n_i$. The massless electron assumption reduces the electron momentum equation to Ohm's law,

$$n_e q_e \mathbf{E} = \nabla p_e - \mathbf{J}_e \times \mathbf{B}. \tag{11}$$

The infinite speed of light assumption reduces Ampere's law to,

$$\mathbf{J} = \frac{1}{\mu_0} \nabla \times \mathbf{B} \tag{12}$$

such that $\mathbf{J}_e = \mathbf{J} - \mathbf{J}_i$. The magnetic field is described by Faraday's law, Eq. (5).

Since infinite speed of light is assumed, the time step for Hall-MHD is restricted by the whistler wave which grows without bound.[2] This unbounded whistler wave results from neglecting electron inertia and its speed is defined by

$$v_W = k \frac{v_A^2}{\omega_{ci}} \tag{13}$$

where $k = \pi/\Delta x$ marks the cut-off for the waves to be resolved in the system.

II.C. Ideal-MHD

Applying further approximations to Hall-MHD leads to Ideal-MHD. The time scales for ideal-MHD are much longer than the time scale of collisions and the ion cyclotron times. The length scales for ideal-MHD are much longer than the ion skin depth and the ion Larmor radius.

The two-fluid effects governed by the Hall term and the electron pressure gradients are not taken into account in ideal-MHD and small-spatial and temporal scale physics is lost. Continuity, momentum and energy are used to describe the single fluid and the induction equation is used to evolve the magnetic field.

II.D. Numerical Method

The results in this paper are obtained using a Runge-Kutta discontinuous Galerkin method with 2nd order accuracy in space and time. The discontinuous Galerkin method,[3] a finite element method, is used to evolve the solution in space. A Runge-Kutta time integration scheme is used to evolve the solution in time explicitly. The two-fluid equations are written in the form of hyperbolic equations with source terms, i.e. *balance laws*.[4,5] The Hall-MHD equations are written using the hyperbolic Euler equations with source terms for the ion fluid. The electron current and electric fields for Hall-MHD however, are evolved using central differencing. In this paper, the electron pressure gradient is assumed to be the same as the ion pressure gradient, i.e. $\nabla p_e = \nabla p_i$ for Hall-MHD.

III. Results

III.A. Electromagnetic plasma shock

An electromagnetic plasma shock is initialized with a gradient in electron and ion densities, pressures and the z-direction magnetic field for the two-fluid plasma model. For Hall-MHD, the ion fluid and magnetic fields are initialized the same way as the two-fluid case. All results for this problem are done using 256 cells with the 2nd order RKDG method.

Figures 1 and 2 show the two-fluid model and Hall-MHD solutions for different ion Larmor radii. At an ion Larmor radius of 7×10^{-1} in Fig. 1, the two-fluid model employs a realistic ion-to-electron mass ratio of

American Institute of Aeronautics and Astronautics
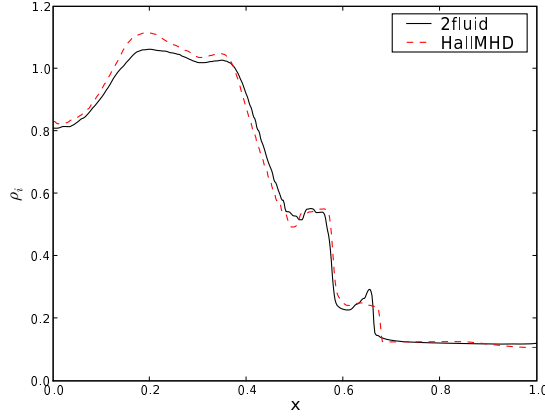
Figure 1. The two-fluid plasma model is compared to Hall-MHD after 0.2 **Alfven transit times for** $r_{Li} = 7 \times 10^{-1}$**. The two-fluid plasma model solution with realistic ion-to-electron mass ratio,** $mi/me = 1836$**, agrees well with the Hall-MHD solution.**
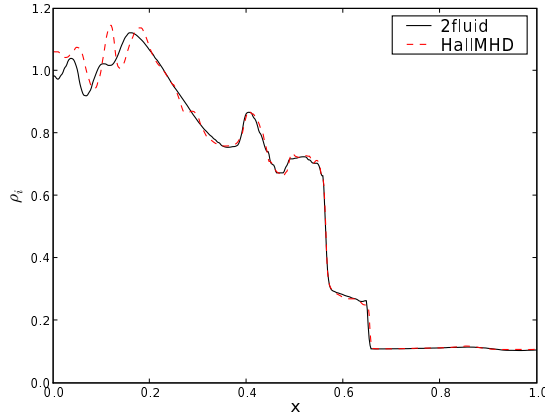
Figure 2. The two-fluid plasma model is compared to Hall-MHD after 0.2 **Alfven transit times for** $r_{Li} = 7 \times 10^{-2}$**. The Hall-MHD solution is similar to the two-fluid plasma model solution with ion-to-electron mass ratio,** $mi/me = 183.6$**. With realistic ion-to-electron mass ratio at this Larmor radius, the problem becomes stiff for the two-fluid model.**

1836. This solution compares well with the Hall-MHD solution that assumes massless electrons. At an ion Larmor radius of 7×10^{-2} in Fig. 2, the two-fluid model becomes stiff if the realistic ion-to-electron mass ratio is used. Hence, $m_i/m_e = 183.6$ is used in this case where the results between the two-fluid model and Hall-MHD compare well. Figure 3 shows a comparison of the Hall-MHD solution to ideal-MHD for an ion Larmor radius of 7×10^{-4}. At this characteristic scale length, the two-fluid plasma model is very stiff and becomes difficult to solve. The Hall-MHD solution has similar qualities to the ideal-MHD solution and it is seen that decreasing the ion Larmor radius approaches the ideal-MHD limit consistent with theory.

The time step for the two-fluid model is restricted by the speed of light which is assumed to be $100v_A$ for this problem. Since the speed of light is assumed infinite in Hall-MHD, the whistler wave speed restricts the time step using the cutoff wave number described previously. Both the two-fluid model and Hall-MHD solutions have the same effective grid resolution. The time step used for the two-fluid model with real ion-to-electron mass ratio for the $r_{Li} = 7 \times 10^{-1}$ case is approximately 100 times larger than the time step used for Hall-MHD leading to 135 times more computational effort to obtain a Hall-MHD solution as compared to the two-fluid model. For the $r_{Li} = 7 \times 10^{-2}$ case, Hall-MHD takes 14 times more computational effort than the two-fluid model to produce comparable results. Hall-MHD is extremely computationally intensive even though it provides results comparable to the two-fluid model when r_{Li} becomes significant. Hall-MHD is also able to provide results comparable to ideal-MHD when r_{Li} becomes very small unlike the two-fluid model which becomes stiff in this regime. However, in regimes where small spatial and temporal scales are

American Institute of Aeronautics and Astronautics
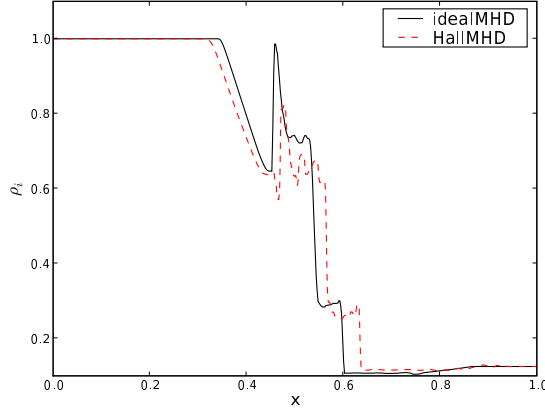
Figure 3. The Hall-MHD model is compared to ideal-MHD after 0.2 Alfven transit times for $r_{Li} = 7 \times 10^{-4}$. At this Larmor radius the two-fluid model becomes too stiff and requires large computational effort to get a solution similar to that of Hall-MHD. The Hall-MHD solution here is compared to the ideal-MHD solution. The solutions have similar qualities but the characteristic speeds seem to vary. It is seen that decreasing the Larmor radius approaches the ideal-MHD limit.

of interest, the two-fluid model is more computationally effective as it uses much less computational effort for this problem compared to Hall-MHD.

III.B. Magnetic reconnection

Magnetic reconnection has been explored using a number of fluid and particle codes due to its role in magnetosphere dynamics, space plasmas and laboratory plasmas. Shay et al.[6] determine that the inclusion of the Hall term is necessary to produce physically correct reconnection rates and Hall-MHD remains the minimum physical model needed to accurately capture magnetic reconnection.

A current sheet is initialized with a density profile of $\text{sech}^2(y)$ and an x-direction in-plane magnetic field profile of $\tanh(y)$. A small initial perturbation is applied to the in-plane magnetic fields in the x- and y-directions. The electron momentum in the z-direction is initialized for the two-fluid model such that it follows the density profile. For Hall-MHD, the electron currents are calculated from the Hall current and the ion fluid velocity. The Hall current is obtained from the curl of the magnetic fields. All results are for a resolution of 128×64 cells using the 2nd order RKDG method with periodic boundary conditions in the x-direction and conducting wall boundaries in the y-direction.
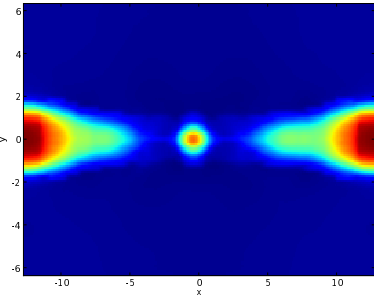
Figure 4. Solution of ion density for the two-fluid model is presented for the magnetic reconnection problem at $\omega_{ci}t = 20$. An island forms in the center of the domain that moves to the left and merges with the plasma.
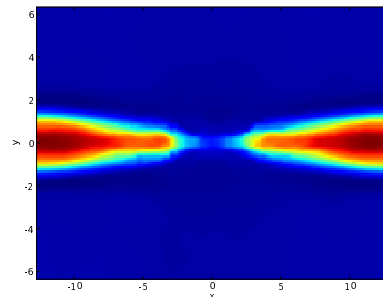
Figure 5. Solution of ion density for Hall-MHD is presented for the magnetic reconnection problem at $\omega_{ci}t = 20$. There is no island formation at the center of the domain with this model.

Figures 4 and 5 show the reconnection at a time of $\omega_{ci}t = 20$ for the two-fluid model and Hall-MHD. The two-fluid model solution of Fig. 4 shows the formation of an island in the center of the domain. This island eventually moves to the left of the domain and begins to merge with the plasma at a time of about $\omega_{ci}t = 33$. The Hall-MHD solution does not have the formation of an island in the center of the domain.

American Institute of Aeronautics and Astronautics
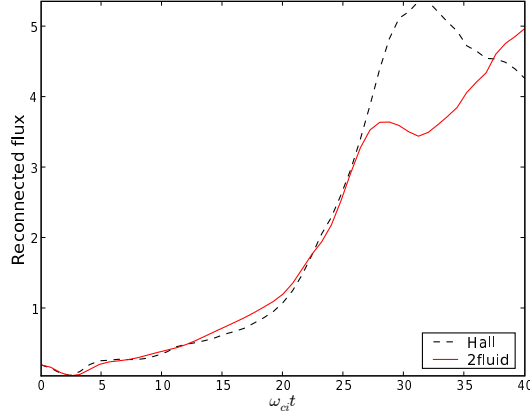
Figure 6. Reconnected magnetic flux is shown as a function of time, $\omega_{ci}t$, for the two-fluid model and Hall-MHD. The reconnection rates match well with previous literature.[6] Hall-MHD reconnects more flux than the two-fluid model before saturating. After the two-fluid model saturates, there is an increase in the reconnected flux again. This increase could be attributed to the merging of the island with the plasma in the left half of the domain.

The reconnected magnetic flux for the two-fluid model and Hall-MHD are shown in Fig. 6. The magnetic flux reconnection rates from this plot agree well with previously published results.[6] The Hall-MHD solution reconnects more flux than the two-fluid model before it saturates. Following reconnection, the two-fluid model saturates briefly and then the flux appears to increase once again. The time when this increase happens correlates with the merging of the island from the center of the domain to the plasma in the left of the domain.

For this problem, the very restrictive time step of Hall-MHD makes it require 15 times the computational effort of the two-fluid model for the same grid resolution and the same initial conditions. Since the reconnection rates of both models match previously published results, the two-fluid model provides the more computationally effective solution.

III.C.   Axisymmetric Z-pinch

An axisymmetric Z-pinch is initialized in two-dimensions using the same parameters, initial conditions, boundary condition implementation and perturbations as Loverich et al.[7] and Srinivasan et al.[8] Axis boundary conditions are implemented in the left edge, conducting wall boundary conditions are implemented in the right edge and periodic boundaries are implemented in the axial direction. A grid of 128×128 cells is used for both models with the 2nd order RKDG method.
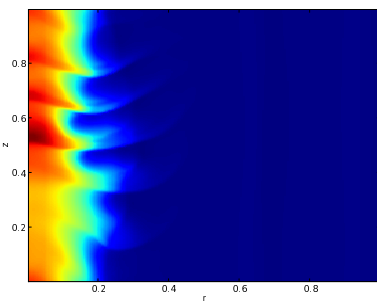
Figure 7. Solution of ion density for the two-fluid model is presented for the axisymmetric Z-pinch problem after 2 Alfven transit times. The short wavelength lower hybrid drift instability grows on top of the single wavelength perturbation.
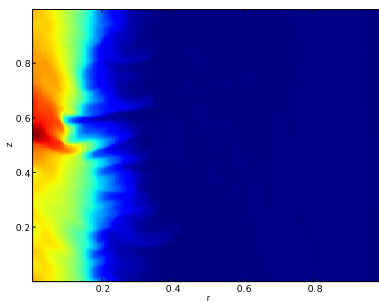
Figure 8. Solution of ion density for Hall-MHD is presented for the axisymmetric Z-pinch problem after 2 Alfven transit times. The short wavelength lower hybrid drift instability grows on top of the single wavelength perturbation just as with the two-fluid solution.

Initializing a single wavelength perturbation initiates the growth of short wavelength perturbations in the solution that correspond to the lower hybrid drift instability as seen in Figs. 7 and 8. The two-fluid and Hall-

American Institute of Aeronautics and Astronautics

MHD solutions have similar qualities in terms of the shapes of the short wavelength modes and the shocks that form in the ion fluid. However, the Hall-MHD solution shows more features in the short-wavelength modes than the two-fluid solution, so the length scales of the lower hybrid drift instability differ between the models. The additional features seen in the Hall-MHD solution could be the result of dispersion of the whistler wave. Both models are able to resolve the lower hybrid drift instability which is a two-fluid effect that results from resolving the ion Larmor radius. The ion Larmor radius is on the order of 1/3 the pinch radius for this problem. Although both models are able to capture small-scale physics, Hall-MHD requires 35 times more computational effort than the two-fluid model for this problem.

IV.   Conclusion

For the electromagnetic shock problem, the results of the two-fluid model and Hall-MHD agree. Ideal-MHD does not capture small-scale physics when the ion Larmor radius becomes significant with respect to the domain size. However, both the two-fluid model and Hall-MHD have similar solutions for larger ion Larmor radii. As the ion Larmor radius becomes very small, the Hall-MHD solution approaches the ideal-MHD solution. At these regimes, the two-fluid model becomes very stiff and requires large computational effort.

The solutions of the two-fluid model and Hall-MHD agree with previously published results for the magnetic reconnection problem. The differences lie in the formation of an additional island in the center of the domain for the two-fluid model solution that eventually moves to the left of the domain and merges with the plasma. No such island forms in the center of the domain for Hall-MHD. The magnetic flux reconnection rates of both models agree although the reconnected magnetic flux for Hall-MHD is larger than the two-fluid model before it saturates.

The formation of the short-wavelength lower hybrid drift instability for the two-dimensional axisymmetric Z-pinch problem is also compared between the two-fluid model and Hall-MHD. Both the models are able to resolve this two-fluid effect that is seen when the ion Larmor radius is resolved. The shapes of the short wavelength modes that arise have similar qualities between the two-fluid model and Hall-MHD although the Hall-MHD solution shows more features than the two-fluid model. Hence, the models differ in the length scales of the lower hybrid drift instability.

It is more computationally expensive to use Hall-MHD versus the two-fluid model for problems involving small spatial scales and short temporal scales. The two-fluid effects at these parameter regimes are captured by both the two-fluid model and Hall-MHD, however, depending on the problem of interest, Hall-MHD takes between 14 and 135 times the computational effort of the two-fluid model for the same effective grid resolution, using the same initial conditions and being solved in the same parameter space.

Acknowledgments

References

[1] U. Shumlak and J. Loverich, *Approximate Riemann solver for the two-fluid plasma model*, Journal of Computational Physics, 187:620–638, 2003.

[2] J. D. Huba, *Hall magnetohydrodynamics – a tutorial*, Space Plasma Simulation, Springer, 2003.

[3] B. Cockburn and C.-W. Shu, *Runge-Kutta discontinuous Galerkin methods for convection-dominated problems*, Journal of Scientific Computing, 16:173–261, 2001.

[4] R. J. LeVeque, *Finite Volume Method for Hyperbolic Problems*, Cambridge University Press, 2002.

[5] A. Hakim, J. Loverich and U. Shumlak, *A high resolution wave propagation scheme for ideal Two-Fluid plasma equations*, Journal of Computational Physics, 219:418–442, 2006.

[6] M. A. Shay, J. F. Drake, B. N. Rogers and R. E. Denton, *Alfvenic collisionless magnetic reconnection and the Hall term*, Journal of Geophysical Research, 106:3759–3772, 2001.

[7] J. Loverich and U. Shumlak, *Nonlinear full two-fluid study of m=0 sausage instabilities in an axisymmetric Z-pinch*, Physics of Plasmas, 13:082310, 2006.

[8] B. Srinivasan, A. Hakim and U. Shumlak, *A comparison of high-resolution wave propagation method and Runge-Kutta discontinuous Galerkin method for plasma fluid equations*, Journal of Computational Physics, To be submitted, 2008.